***JKPK (JURNAL KIMIA DAN PENDIDIKAN KIMIA)**, Vol. 7, No. 3, 2022* *pp. 287-302*
Chemistry Education Study Program, Universitas Sebelas Maret *ISSN 2503-4146*
https://jurnal.uns.ac.id/jkpk *ISSN 2503-4154 (online)*

^{1}H and ^{13}C NMR STUDY OF OLIGOSUCCINIMIDE PREPARED BY THERMAL CONDENSATION AND EVALUATION OF ITS SCALE INHIBITION

Muhamad Jalil Baari [1,*] Megawati [1], and Didi Prasetyo Benu [2]

[1]Department of Chemistry, Faculty of Sciences and Technology, Universitas Sembilanbelas November Kolaka, Southeast Sulawesi Indonesia
Jl. Pemuda, Tahoa, Kolaka, Southeast Sulawesi, Indonesia
[2]Department of Chemistry, Faculty of Agriculture, Universitas Timor, Timor Tengah Utara, Indonesia
Jl. El Tari - Km. 09,Timor Tengah Utara, East Nusa Tenggara, Indonesia

* Correspondence, email: jalilbaari@gmail.com

Received: September 23, 2022 Accepted: December 5, 2022 Online Published: December 11, 2022
DOI : 10.20961/jkpk.v7i3.65666

ABSTRACT

The presence of scale is a serious problem in the petroleum industry, and some efforts should be made to control scale formation. Oligosuccinimide (OSI) is an oligomer with several repeating units of succinimide. The structure of the OSI main chain and end groups has never been comprehensively analyzed. Meanwhile, OSI is potentially a scale inhibitor due to chelating properties, high polarity, and high solubility. This study investigates the molecular structure of oligosuccinimide, focusing on the main chain and end groups. Synthesis was carried out by thermal condensation between maleic anhydride and ammonium carbonate using a ^{1}H and ^{13}C NMR spectroscope equipped with Distortionless Enhancement by Polarization Transfer 135, Heteronuclear Multiple Quantum Coherence, and Single Quantum Coherence. The NMR analysis results detected the presence of the main chain and several synthesized OSI end groups, such as the amino, succinimide, and maleimide end groups. However, the dicarboxylic acid end group and other irregular structures, as in polysuccinimide (various synthesis methods), were not identified. It confirmed that our thermal condensation method produced OSI with less irregular structures than previous methods. Evaluation of OSI as $CaCO_3$ and $CaSO_4$ scales inhibitor showed reasonably good performance in very small concentrations. The inhibition efficiency was 73.20% for the $CaCO_3$ scale with 10 mg.L^{-1} and 55.29% for the $CaSO_4$ scale with 10 mg.L^{-1} inhibitor concentration. Analysis of thermal stability informed OSI has good thermal stability because it started to be degraded at 353.38 °C.

Keywords: *oligosuccinimide, thermal condensation, $CaCO_3$, $CaSO_4$, scale inhibitor*

INTRODUCTION

Nowadays, the efforts to produce scale formation in petroleum industries keep going. It relates to the technical and environmental issues from the accumulation of calcium, sulfate, and carbonate ions to form calcium carbonate ($CaCO_3$) and calcium sulfate ($CaSO_4$) scales. Scales are usually found in the transportation stage of oil and gas through pipelines because the transported fluids carry not only oil and gas but also seawater which contains salt or inorganic ions, dissolved gasses, and microorganisms. These scales lead to

problems such as blockage of drain pipes, pitting corrosion, reduction of hydrocarbon production, and the cessation of industrial operations [1,2]. Pitting corrosion is the main factor for pipeline leakage [3].

Consequently, oil spills hurt organisms' survival and interfere with environmental sustainability. Thus, a way is needed to control or minimize the reactions of scale formations. There are physical methods, such as applying ultrasonic waves and magnetic fields [4,5]. However, it needs a higher cost. Another method that is quite effective for preventing scale formation is acidification with an acid solution [6]. However, this method also increases the corrosion rate on pipelines made from metal. Using scale inhibitors is a practical, economical, and safer way for the environment [1]. The chemical reaction between the scrimpy concentration of scale inhibitors and inorganic ions/salts can inhibit the deposition process on the inner surface of the pipeline.

Polisuccinimide (PSI) is a biodegradable compound [7], but it can only dissolve in organic solvents like dimethylformamide (DMF) which has the potency to damage the environment [8]. These chemical properties limited PSI use for some applications, especially corrosion and scale inhibitors. The chemical structure of PSI has been analyzed [9,10]. There are a lot of irregular structures in the main chain and end groups. Meanwhile, PSI derivatives/modified PSI have been used as corrosion and scale inhibitors [6,11]. It was also used as a cleaning agent in wastewater treatment. This usage relates to the nature of PSI derivatives/modified PSI, for instance, good dispersion capacity and the ability as a chelating agent to prevent the deposition of calcium carbonate, calcium phosphate, and calcium sulfate salts. PSI is hydrolyzed with robust base solutions like sodium hydroxide to form sodium polyaspartates and derivatives/modified PSI [11-14]. Then, it continued with chemical reactions with other substances. PSI modification requires chemicals like NaOH, HCl, $FeSO_4.7H_2O$, $CuSO_4.5H_2O$, H_2SO_4, H_3PO_4, etc. [6,11,15]. Thus, cost requirements and chemical waste also increase.

Reducing the length of PSI chains into their oligomeric forms increases their polarity and water solubility [16]. The presence of functional groups in OSI was characterized using a Fourier Transform Infrared (FTIR) spectrometer. At the same time, Liquid Chromatography-Mass Spectroscopy (LC-MS) analyzed oligomer fractions and their mass. However, a comprehensive analysis of the OSI main chain and end groups has not been carried out yet. Therefore, this study used NMR characterization to analyze OSI primary and irregular (end groups) structures.

Besides that, OSI is known to be quite effective in reducing the corrosion rate of carbon steel [16]. Corrosion inhibition efficiency above 60% indicates physical and chemical interactions between OSI molecules and iron atoms in steel. The presence of heteroatoms/functional groups and water solubility property affects its performance. Hence, this research is based on considerations of the capability of OSI compound to interact with alkali metal ions

such as calcium ions (Ca^{2+}) to prevent scales formation. OSI is expected to be effective as a scale inhibitor. Thus, it has a dual function as a corrosion and scale inhibitor. Consequently, the use of acidic compounds will be reduced. The thermal analysis of OSI was also conducted to observe when OSI begins to degrade because thermal stability is an essential factor for applying scale inhibitors.

METHODS

Materials and Instruments

Materials used in this study were ammonium carbonate (Merck), maleic anhydride (Merck), absolute ethanol (Merck), demineralized water, calcium chloride dehydrate (Merck), sodium sulfate (Merck), ethylene diamine tetraacetic acid (Merck), sodium bicarbonate (Merck), buffer pH 12, silicone oil, and Eriochrome black T. All used reagents did not undergo further purification. The instruments used in this study consist of laboratory glassware, reflux apparatus, vacuum pump, Buchner funnel, vacuum oven, Bruker Avance 500 MHz for ^{1}H NMR and 125 MHz for ^{13}C NMR spectrophotometers equipped by DEPT, HSQC, and HMQC in D_2O, NETZSCH STA 449F1 instrument for Thermogravimetric Analysis, Memmert oven.

Synthesis of Oligosuccinimide (OSI)

The synthesizing procedure of oligosuccinimide was adopted by Baari et al. [16]. First, mix 6.53 grams of maleic anhydride in demineralized water and 7.69 grams of ammonium carbonate, which was also dissolved in demineralized water. Next, the mixture was refluxed for 1 hour at 180 °C. After that, it evaporated until an orange solid formed. The resulting solid was washed with absolute ethanol and dried in a vacuum oven at 65 °C for 24 hours. Furthermore, the obtained OSI was placed in a desiccator to keep it dry.

Analysis of Molecular Structure

Functional groups and the number of repeating units of OSI have been previously characterized by FTIR and LC-MS spectra [16]. Types of hydrogen and carbon were characterized by ^{1}H NMR, ^{13}C NMR, and Distortionless Enhancement by Polarization Transfer (DEPT 135). Heteronuclear Multiple Quantum Coherence (HMQC) and Single Quantum Coherence (HSQC) spectra investigated the correlation between protons and carbons. The NMR instrument used in this study is Bruker Avance 500 MHz for ^{1}H NMR and 125 MHz for ^{13}C NMR in D_2O.

$CaCO_3$ Scale Inhibition

The efficiency of $CaCO_3$ scale inhibition by oligosuccinimide solution was measured using a static $CaCO_3$ precipitation procedure according to the Chinese Standard Method GB/T 16632-2008. The step was initiated by making calcium (Ca^{2+}) and carbonate (CO_3^{2-}) solutions as a source of $CaCO_3$ scale. The Ca^{2+} solution was made from $CaCl_2.2H_2O$, while the CO_3^{2} solution was made from $NaHCO_3$ at a similar concentration of 250 $mg.L^{-1}$. Then, both solutions were mixed in testing bottles at the same ratio to analyze the inhibition efficiency with and without the addition of an inhibitor [17].

$CaSO_4$ Scale Inhibition

This test is almost similar to the inhibition efficiency test of the $CaCO_3$ scale. It was based on the formation of a $CaSO_4$

precipitate. The solutions of calcium (Ca^{2+}) and sulfate (SO_4^{2-}) were used as a source of the $CaSO_4$ scale. Ca^{2+} solution was made from $CaCl_2.2H_2O$, while SO_4^{2-} the solution was made from Na_2SO_4 with equal concentrations of 6800 $mg.L^{-1}$. Greater concentrations are used because $CaSO_4$ is more water soluble than $CaCO_3$. Both solutions were mixed at the same ratio in tested bottles to analyze the inhibition efficiency with and without the addition of an inhibitor [18,19].

Calculation of Inhibition efficiency by complexometry titration

Each brine solution was divided into blank solutions, and the solutions with the addition of oligosuccinimide at various concentrations of 2, 4, 6, 8, to 10 ppm. First, blank solutions were divided into unheated (B1) and heated blank (B2) solutions. Then, 10 mL of unheated blank (B1) was poured into the Erlenmeyer flask, added buffer solution (pH 12) and EBT indicator, and titrated with EDTA solution. Meanwhile, the blank (B2) and brine solutions with the addition of inhibitor were heated in an oven at 80 °C for 24 hours. After that, the tested brine solution was placed at ambient temperature before titrating with EDTA solution, following the previous steps. The remained calcium ion concentrations ($[Ca^{2+}]$), and inhibition efficiencies of the inhibitor were calculated using Equations 1 and 2 below [12,20].

$$[Ca^{2+}] = \frac{M_{EDTA} \cdot V_{EDTA}}{V_{system}} \quad (1)$$

$$IE = \frac{[Ca^{2+}]_A - [Ca^{2+}]_{B2}}{[Ca^{2+}]_{B1} - [Ca^{2+}]_{B2}} \times 100\% \quad (2)$$

Where $[Ca^{2+}]_{B1}$ and $[Ca^{2+}]_{B2}$ are calcium ion concentrations of the brine solutions without inhibitor for unheated and under heated, respectively. M_{EDTA} is EDTA molarity (M), V_{EDTA} is the volume of EDTA (mL), $[Ca^{2+}]_A$ is calcium ion concentration with the presence of inhibitor, and V_{system} is the volume of tested brine solution.

Thermal Stability Analysis

The thermal stability of synthesized OSI was analyzed using the Thermogravimetric Analysis Method (TGA) using the NETZSCH STA 449F1 instrument. The range of temperature is 25 – 500 °C. The temperature rise rate was 10 °C/min under the nitrogen gas atmosphere.

RESULTS AND DISCUSSION

The reaction scheme and mechanism of oligosuccinimide production from maleic anhydride and ammonium carbonate as precursors are displayed in Figure 1 and Figure 2, respectively. This method did not use organic solvents to minimize the accumulation of chemical waste. Instead, the reactions occur in the functional groups of both precursors as the feature of condensation reaction [16].

Figure 2 displays the formation of maleic acid after hydrolyzing maleic anhydride. At the same time, it hydrolyzes ammonium carbonate to ammonium ions which are in equilibrium with ammonia. Those species then react to form OSI. Irregular structures in the end groups of synthesized OSI may occur due to other mechanisms during reactions. The molecular structure of OSI was comprehensively analyzed by NMR spectroscopy.

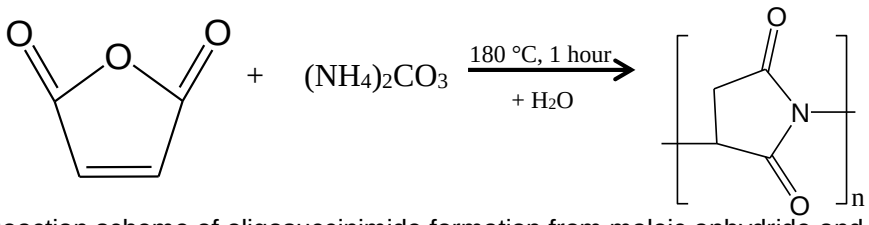

Figure 1. Reaction scheme of oligosuccinimide formation from maleic anhydride and ammonium carbonate [16]

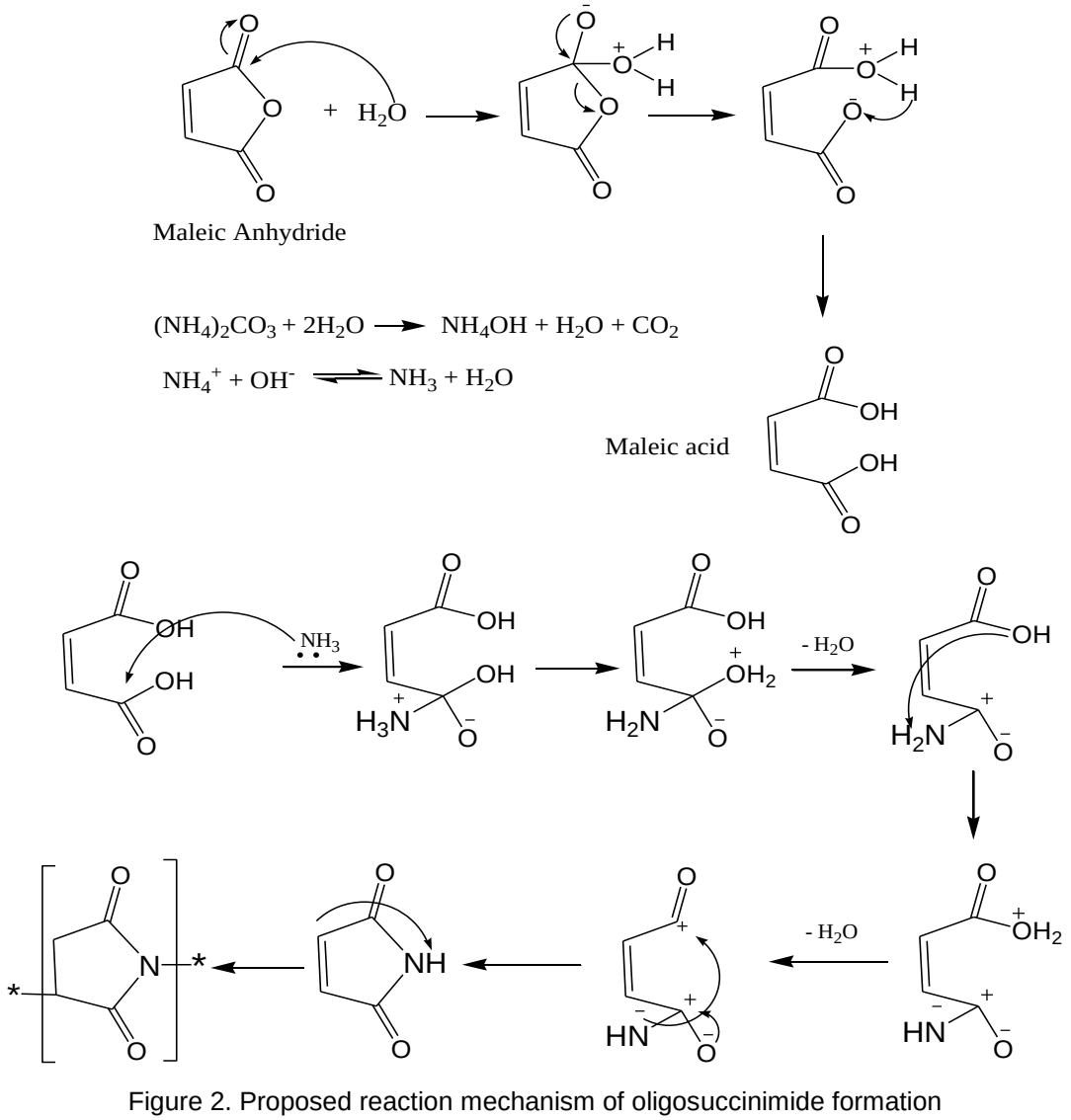

Figure 2. Proposed reaction mechanism of oligosuccinimide formation

Characterization of Nuclear Magnetic Resonance Spectroscopy (^{1}H NMR, ^{13}C NMR, DEPT 135, HMQC, HSQC)

The 500 MHz, ^{1}H NMR spectra of oligosuccinimide in D_2O are shown in Figure 3. Several peaks and their chemical shift display several proton types in the OSI compound. Methylene protons usually appear more upfield than methine at ^{1}H NMR spectra due to being more shielded. The chemical shifts of methylene protons are about 2.68-2.82 ppm, whereas the peaks of

methine protons appear at about 3.8-3.85 ppm. The signals in 6.15 and 6.50 ppm relate to double-bond protons in maleimide end groups. Then, triplet and quartet peaks at 0.9-1.02 ppm and 3.45-3.50 ppm correspond to the incorporation of ethyl alcohol that strongly interacted with OSI chains. HSQC spectra display those protons relate to methyl carbon (C-14*) and methylene carbon (C-15*) at 16.70 and 57.30 ppm, respectively.

Meanwhile, The signal around 4.65 ppm shows the solvent's undeuterated part and the water hydrate's presence in the oligomer exposed when the OSI was dissolved. These spectra arise owing to the exchangeable nature of amines or amides protons [21]. Therefore, using D_2O as a solvent could negate the proton spectra of amines or amides.

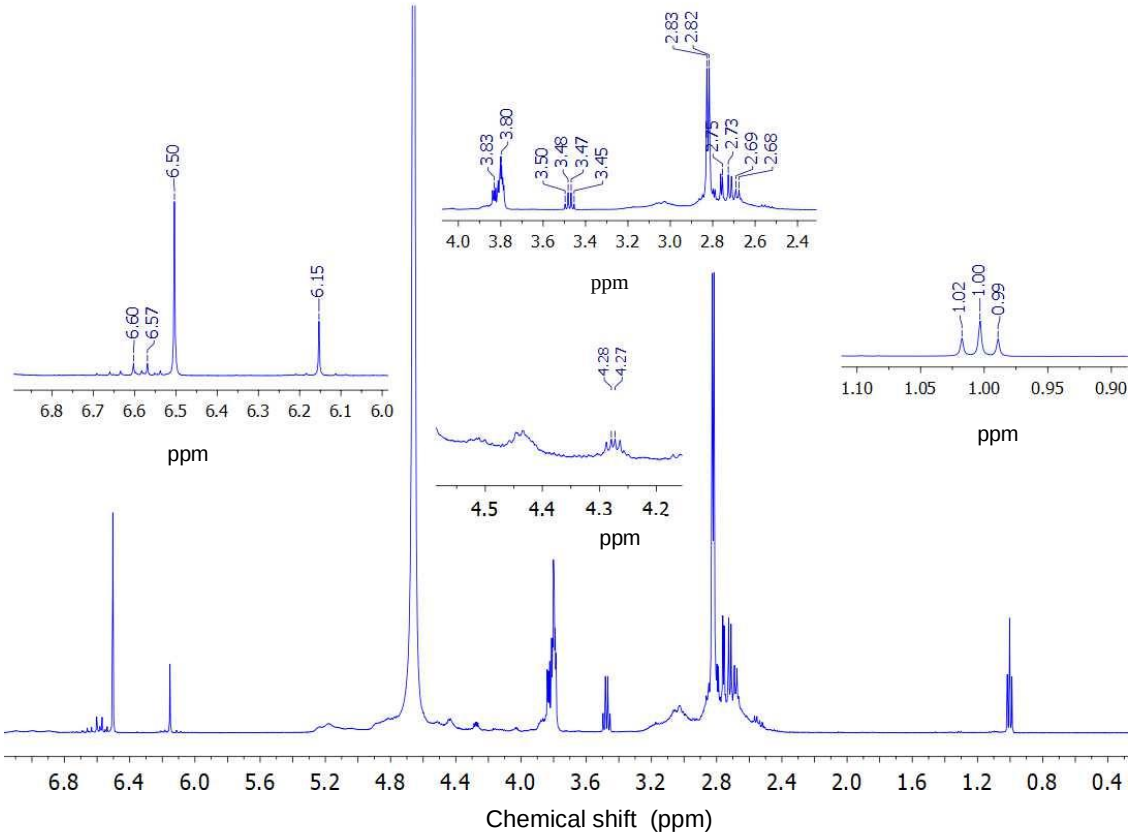

Figure 3. ^{1}H NMR spectra of OSI (in D_2O solvent)

Then, the types and distinctions of carbon (methylene, methine, or carbonyl carbon) contained in the OSI structure were determined by ^{13}C NMR and DEPT 135 in Figures 4a and 4b. Face-down signals relate to methylene carbon, while methine and double-bond carbons signal face-up [22]. The difference is in chemical shifts, in which double-bond carbons appear more downfield (more significant chemical shift). The results of the DEPT 135 analysis show that carbonyl carbon is not detected because there is no proton bonded as a transferring polarization

species to produce magnetization and increase the intensity of carbon signals [23].

Furthermore, the correlations of protons and carbons at a distance of one bond or bind directly are specified by 2-D NMR spectra (HMQC and HSQC) in Figures 12 and 13. Besides DEPT 135, HMQC and HSQC tests inform types of carbons that bind protons and also without attaching protons. These tests correlate proton-carbon signal frequencies in one bond [22]. A carbon without a proton can be classified as a quarternary or carbonyl (except aldehydes) carbon. Meanwhile, signals in ^{1}H NMR from proton and oxygen or nitrogen atoms will not appear in HMQC or HSQC spectra. HSQC spectra present contours related to CH_3, CH_2, and CH groups. CH_3 and CH groups have similar contour colours (blue-red). The difference is in the chemical shifts due to the shielding effect. Meanwhile, the CH_2 group has red-blue contour colour.

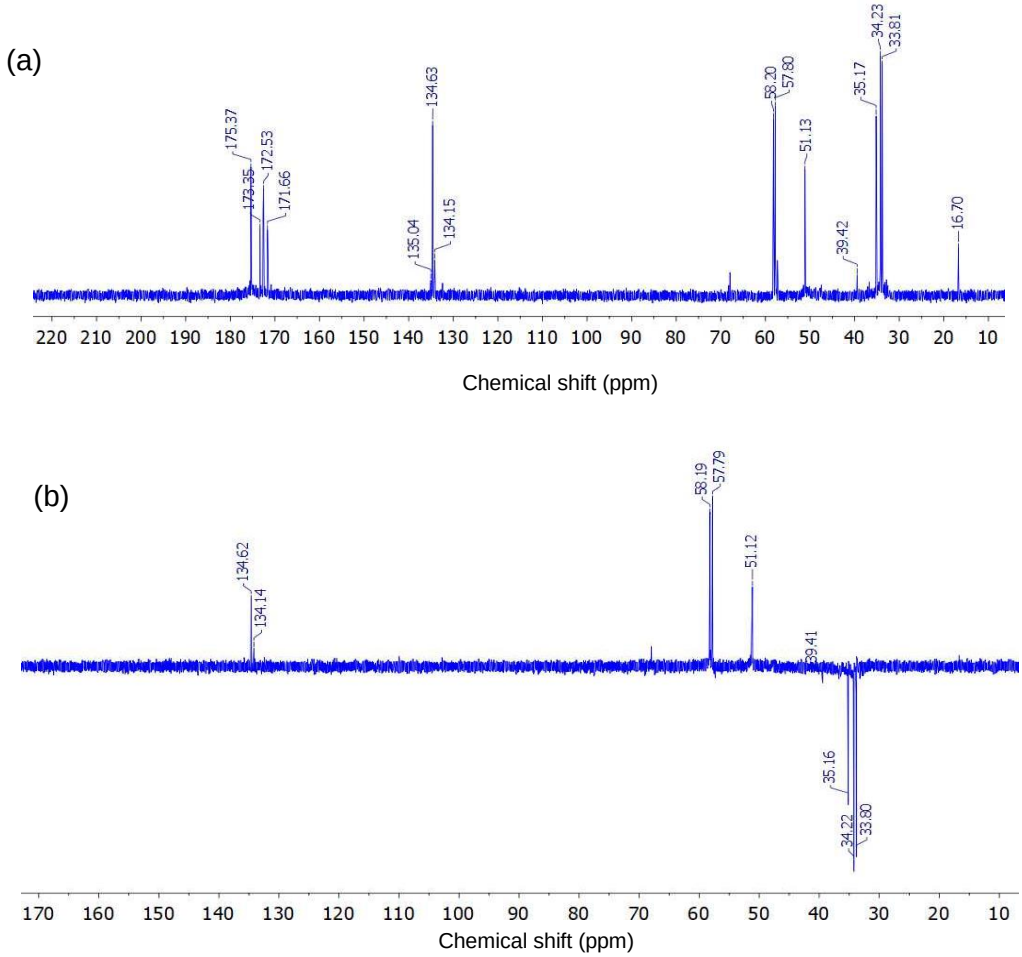

Figure 4. ^{13}C NMR spectra (a) and DEPT 135 spectra (b) of OSI in D_2O

Table 1 summarizes chemical shift values of carbons and relations between proton-carbon based on NMR spectra, primary chain, and types of end groups of synthesized OSI.

Structure of Main Chain

The presence of signals in 2.83 ppm relates to protons (H-6) that directly bonded to methylene carbons (C-6) at 34.66 ppm.

Then, the proton at 3.88 ppm (H-5) corresponds to methine carbon at 57.91 ppm (C-5). The signals of methine protons and carbons were detected at more significant chemical shifts because their nuclei were de-shielded than methylene protons and carbons [21]. There are several carbon signals from four carbonyl carbons with different chemical environments. The difference in resonance frequency around the magnetic field between rings in the middle or main chain and rings in the end groups of the OSI structures inflicts slightly different chemical shifts of carbonyl carbon signals. Carbonyl carbons (C-8 and C-10) signals in the main chain of OSI appear at 172.53 and 171.66 ppm. These signals appear at larger chemical shifts because carbonyl carbons were de-shielded after bonding to the oxygen atoms [21,24]. The inductive effect from oxygen atoms leads to a decrease in electron density. HSQC spectra confirm no traces between carbon and protons for signals in the range 171.66 – 175.37 ppm [23]. Generally, these spectra are similar to NMR spectra of polysuccinimide in DMSO-d_6 solvent [9,10]. The slight distinction lies in the chemical shifts of the signals/peaks.

End Groups

The end groups of synthesized OSI are pretty interesting to be analyzed. It corresponds to several types of end groups in the OSI structure. Figure 5 shows the typical OSI structure, the amino end group, the dicarboxylic acid end group, the succinimide end group, and the maleimide end group, which may be formed based on the NMR spectrum. Because D_2O was used as a solvent in NMR analysis, thus proton signal of amine in the amino end group or amide in the succinimide end group did not appear. Meanwhile, the main chain's proton signals of methylene and methine are slightly different from proton signals in succinimide and maleimide end groups. The chemical shifts of proton signals in the succinimide end group are more upfield because their nuclei are more shielded than the middle chain. Higher electron density generates more protected nuclei [21]. However, carbonyl carbons (C-1 and C-2) in the succinimide end group have more downfield signals at 175.37 and 173.35 ppm [10].

Table 1. Chemical shifts of types ^{1}H and ^{13}C based on NMR spectra of oligosuccinimide

Mark from figure 5	^{1}H chem.shift, δ_H (ppm)	^{13}C chem.shift, δ_C (ppm)	Mark from figure 5	^{1}H chem.shift, δ_H (ppm)	^{13}C chem.shift, δ_C (ppm)
1	–	175.37	9	3.84	58.58
2	–	173.35	10	–	171.66
3	3.85	51.21	11	6.10	134.15
4	2.75	35.13	12	6.50	134.63
5	3.88	57.91	13	2.68	36.78
6	2.83	34.66	14*	1.00	16.70
7	4.27	67.96	15*	3.48	57.30
8	–	172.53			

*: Mark for incorporated ethyl alcohol

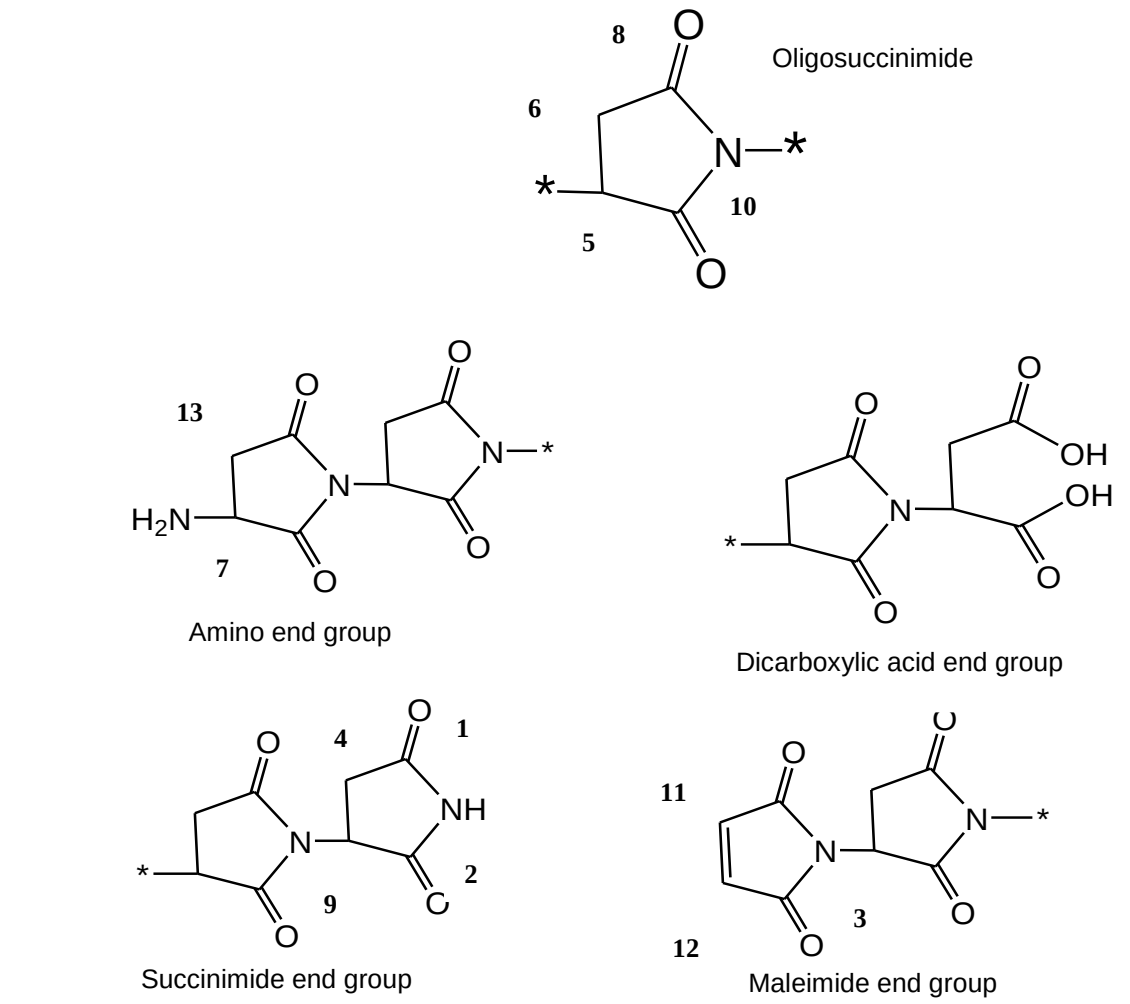

Figure 5. End group possibilities of OSI structure.

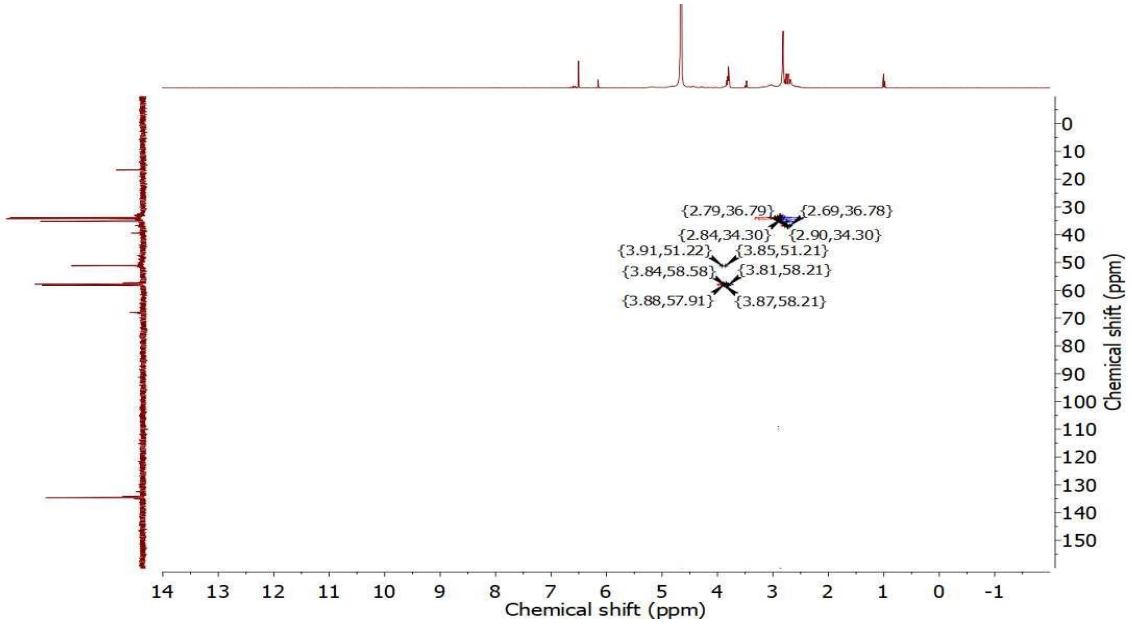

Figure 6. HMQC Spectra of oligosuccinimide

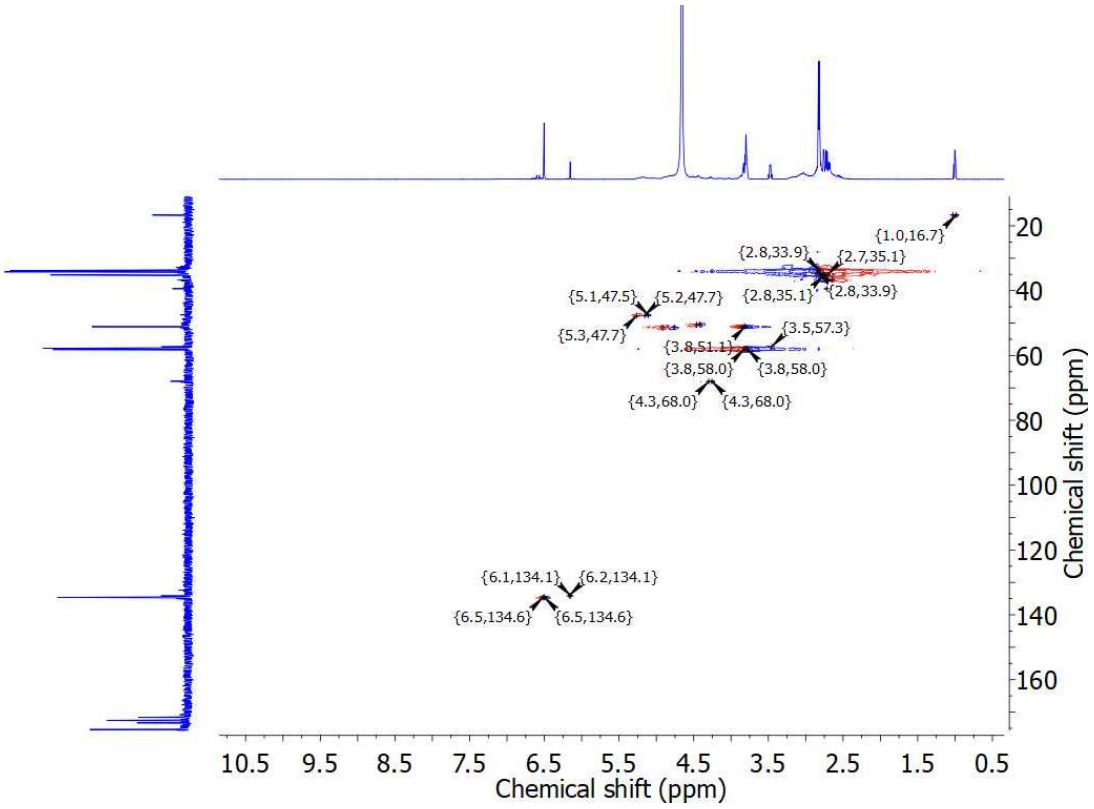

Figure 7. HSQC Spectra of oligosuccinimide

Protons (H-11 and H-12) at 6.1 and 6.5 ppm in the maleimide end group are bonded to carbons (C-11 and C-12) at 134.15 and 134.63 ppm, respectively, based on HSQC spectra. Therefore, these carbons and protons have more downfield signals than others due to the anisotropy effect from the presence of double bonds. In addition, double bonds affect downfield nuclei resonances and produce an electron magnetic field that adds an applied magnetic field near protons. Thus, making their nuclei de-shielded [21].

Inhibition Performance of Oligosuccinimide against $CaCO_3$

The performance of OSI as a scale inhibitor was analyzed through a static scale inhibition test. Table 2 displays the scale inhibition test of OSI in various concentrations against $CaCO_3$. OSI has a good performance as a scale limiter. The electronegative atoms (nitrogen and oxygen) in amide functional groups of OSI can adsorb till forming coordination bonds with calcium ions via lone pair electrons. Therefore, scale formation in an aqueous solution was inhibited. Besides that, the crystal growth after the salt nucleation process was retarded due to interparticle repulsive force [17,25]. The inhibition efficiency increased by increasing the inhibitor concentration to 10 $mg.L^{-1}$. It relates to the more interactions between OSI molecules and calcium ions for preventing $CaCO_3$ aggregates in the solution. $CaCO_3$ scale inhibition efficiency of OSI reached 73.2% at 10 $mg.L^{-1}$. This inhibition efficiency is better than several polyaspartic acids in other studies (Table 4). This value may continue to rise with increasing OSI concentration.

Table 2. $CaCO_3$ scale inhibition efficiency of OSI in different concentrations

Concentration ($mg.L^{-1}$)	The average volume of EDTA (mL)	$[Ca^{2+}]$ ($mol.L^{-1}$)	IE (%)
0 ppm (unheated)	6.03	0.000603	-
0 ppm (heated)	3.68	0.000368	-
2	3.93	0.000393	10.64
4	4.05	0.000405	15.74
6	4.30	0.000430	26.38
8	4.40	0.000440	30.64
10	5.40	0.000540	73.20

Inhibition Performance of Oligosuccinimide Against $CaSO_4$

$CaSO_4$ is also a common type of scale in petroleum pipelines. Preventing this scale formation needs to be conducted for a sustainable production system. The results of the $CaSO_4$ scale inhibition analysis are presented in Table 3. Similar to $CaCO_3$ inhibition efficiency, the inhibition performance of OSI against the $CaSO_4$ scale also increased with the rising OSI concentration. The optimum inhibition efficiency is 55.29% at the concentration of 10 $mg.L^{-1}$. The presence of polar groups and lone pair electrons hindered the crystallization and crystal growth of $CaSO_4$ through adsorption until the chelation of OSI molecules to Ca^{2+} ions. Thus, OSI fairly effectively inhibits $CaSO_4$ scale formation. However, in other studies, this inhibition efficiency is lower than poly aspartic acid.

Table 3. $CaSO_4$ scale inhibition efficiency of OSI in different concentrations

Concentration ($mg.L^{-1}$)	The average volume of EDTA (mL)	$[Ca^{2+}]$ ($mol.L^{-1}$)	IE (%)
0 ppm (unheated)	15.43	0.001543	-
0 ppm (heated)	7.20	0.00720	-
2	8.07	0.00807	10.57
4	8.58	0.00858	16.77
6	9.38	0.00938	26.49
8	10.10	0.001010	35.24
10	11.75	0.001175	55.29

Inhibitors in small concentrations were used in this study to investigate the effectiveness and efficiency of OSI as $CaSO_4$ and $CaCO_3$ scale inhibitors. The results show OSI has worked at 2 ppm of concentration. Even if inhibition efficiency is relatively low, the increase in inhibition efficiency occurs at higher concentrations because there will be more chemical interactions between OSI molecules and calcium ions to inhibit $CaCO_3$ and $CaSO_4$ aggregates in the solution.

Table 4. The inhibition efficiency of poly aspartic acid against $CaCO_3$ and $CaSO_4$ scales in several studies

Inhibitor	Scale: Concentration, Temperature, Testing time	IE	Ref.
Polyaspartic acid	❖ $CaCO_3$: 1 mg.L^{-1}, 80 °C, 6-16 hours ❖ $CaSO_4$: 4 mg.L^{-1}, 80 °C, 6 hours	❖ 99.9% ❖ 90%	[15]
Polyaspartic acid	❖ $CaCO_3$: 8 mg.L^{-1}, 80 °C, 10 hours	❖ 68%	[14]
Polyaspartic acid	❖ $CaCO_3$: 4 mg.L^{-1}, 80 °C, 10 hours	❖ 93%	[12]
Polyaspartic acid	❖ $CaCO_3$: 50 mg.L^{-1}, 80 °C, 8 hours, ❖ $CaSO_4$: 6 mg.L^{-1}, 70 °C, <5 hours,	❖ 50% ❖ 100%	[25]
Polyaspartic acid	❖ $CaCO_3$: 8 mg.L^{-1}, 80 °C, 10 hours ❖ $CaSO_4$: 16 mg.L^{-1}, 70 °C, 10 hours	❖ 97.1% ❖ 100%	[11]
Polyaspartic acid	❖ $CaSO_4$: 5 mg.L^{-1}, 80 °C, 10 hours	❖ 90%	[18]
Polyaspartic acid	❖ $CaCO_3$: 10 mg.L^{-1}, 80 °C, 8 hours ❖ $CaSO_4$: 4 mg.L^{-1}, 80 °C, 8 hours	❖ 63% ❖ 82%	[26]
Oligosuccinimide	❖ $CaCO_3$: 10 mg.L^{-1}, 80 °C, 24 hours ❖ $CaSO_4$: 10 mg.L^{-1}, 80 °C, 24 hours	❖ 73.2% ❖ 55.3%	current study

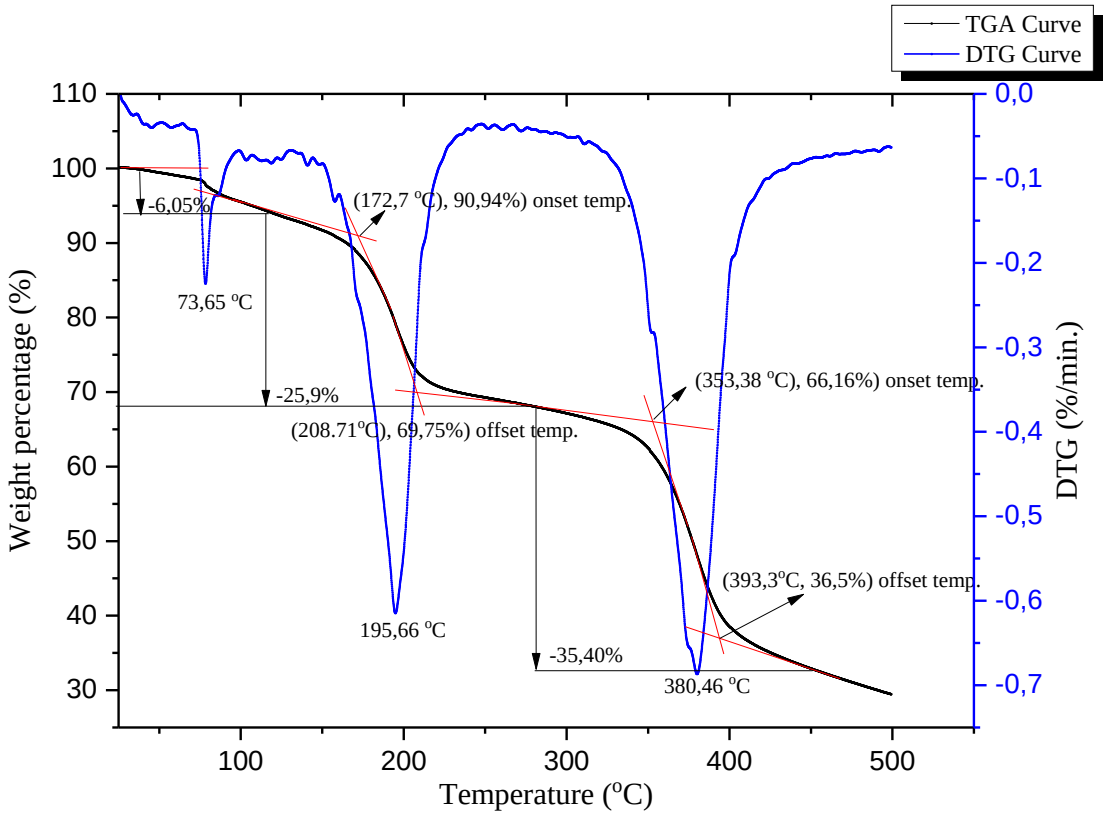

Figure 8. TGA-DTG curves of OSI at 25 – 500 °C, the temperature rise rate = 10 °C/min under the N_2 gas atmosphere

Thermal Stability Analysis

The thermal stability of OSI was analyzed by Thermogravimetric Analysis (TGA). The TGA-DTG curves show that OSI undergoes three stages of decomposition. First stage deals with the loss of volatile molecules and physically adsorbed water at temperatures below 100 °C [27]. These substances have the weakest interaction with OSI molecules. The second stage shows the

release of internal water molecules in the OSI structure at 172.7 – 208.71 °C [28]. There were 25.9% absorbed water molecules in the OSI weight due to this compound's hygroscopic nature. Then, the third stage shows that the OSI molecules begin to decompose at 353.38 °C. It means that OSI will be stable until the ambient temperature reaches 353.38 °C and has not been degraded to 80 °C. This value is lower than polysuccinimide (PSI), which has thermal stability up to 400 °C [29,30].

CONCLUSION

Oligosuccinimide was synthesized by condensation reaction using the reflux method. Structures of the synthesized compound have been analyzed comprehensively through ^{1}H and ^{13}C NMR spectroscopy. NMR spectra of OSI resemble the NMR spectra of PSI with slight differences in chemical shifts. The results informed the main structure and several types of end groups like amino, succinimide, and maleimide end groups. The number of end groups is fewer than in previous synthesis methods. It is related to using water as a solvent in the reaction. The different chemical environment of protons or carbons generates various chemical shifts of the signals in NMR spectra. The induction effects from electronegative atoms and the allotropy effect are the main reason for shield and de-shielded conditions. The study of scale inhibition reveals that OSI can inhibit scale formation in the brine solution. Inhibition efficiency is 73.20% for the $CaCO_3$ scale with 10 $mg.L^{-1}$, reaching 55.29% for the $CaSO_4$ scale with 10 $mg.L^{-1}$ inhibitor concentration. These values are higher than several PASPs in other studies but are lower than modified or PSI/PASP derivatives. Thermal stability was investigated by thermogravimetric analysis. There are three stages of OSI decompositions from TGA/DTG curves. OSI started to be degraded at 353.38 °C.

ACKNOWLEDGEMENT

The Authors would like to thank Direktorat Sumber Daya, Direktorat Jenderal Pendidikan Tinggi, Kementerian Pendidikan, Kebudayaan, Riset, dan Teknologi for funding this research to completion on Basic Research Scheme in 2022.

REFERENCES

[1] M. S. Kamal, I. Hussein, M. Mahmoud, A. S. Sultan, and M. A. S. Saad, "Oilfield scale formation and chemical removal: A review," *J. Pet. Sci. Eng.*, vol. 171, no. January, pp. 127–139, 2018, doi: 10.1016/j.petrol.2018.07.037.

[2] M. J. Baari, B. Bundjali, and D. Wahyuningrum, "Performance of *N,O*-Carboxymethyl Chitosan as Corrosion and Scale Inhibitors in CO_2 Saturated Brine Solution," *Indones. J. Chem.*, vol. 21, no. 4, p. 954, May 2021, doi: 10.22146/ijc.64255.

[3] Y.-H. Lee, G.-I. Kim, K.-M. Kim, S.-J. Ko, W.-C. Kim, and J.-G. Kim, "Localized Corrosion Occurrence in Low-Carbon Steel Pipe Caused by Microstructural Inhomogeneity," *Materials (Basel).*, vol. 15, no. 5, p. 1870, Mar. 2022, doi: 10.3390/ma15051870.

[4] Y. Chen, S. Sun, Y. Lai, and C. Ma, "Influence of ultrasound to convectional heat transfer with fouling of cooling water," *Appl. Therm. Eng.*,

2016, doi:10.1016/j.applthermaleng.2016.01.144.

[5] Y. Han, C. Zhang, L. Wu, Q. Zhang, L. Zhu, and R. Zhao, "Influence of alternating electromagnetic field and ultrasonic on calcium carbonate crystallization in the presence of magnesium ions," *J. Cryst. Growth*, 2018, doi: 10.1016/j.jcrysgro.2018.07.037.

[6] C. Chai, Y. Xu, Y. Xu, S. Liu, and L. Zhang, "Dopamine-modified polyaspartic acid as a green corrosion inhibitor for mild steel in acid solution," *Eur. Polym. J.*, vol. 137, no. April, p. 109946, 2020, doi:10.1016/j.eurpolymj.2020.109946

[7] Z. Liu, Y. Sun, X. Zhou, T. Wu, Y. Tian, and Y. Wang, "Synthesis and scale inhibitor performance of polyaspartic acid," *J. Environ. Sci.*, vol. 23, pp. S153–S155, Jun. 2011, doi:10.1016/S1001-0742(11)61100-5.

[8] D. Zhu, J. Guo, P. Yang, L. Pan, X. Zhong, and S. Chen, "Synthesis and characterization of polyaspartic acid-glutamic acid grafted copolymers and their performances as detergent builder," *J. Appl. Polym. Sci.*, vol. 131, no. 10, p. n/a-n/a, May 2014, doi: 10.1002/app.40282.

[9] K. Matsubara, T. Nakato, and M. Tomida, "1H and 13C NMR characterization of poly(succinimide) prepared by thermal polycondensation of L-aspartic acid," *Macromolecules*, vol. 30, no. 8, pp. 2305–2312, 1997, doi: 10.1021/ma961579h.

[10] M. Piątkowski, D. Bogdał, and K. Raclavský, "1H and 13C NMR Analysis of Poly(succinimide) Prepared by Microwave-Enhanced Polycondensation of L-Aspartic Acid," *Int. J. Polym. Anal. Charact.*, vol. 20, no. 8, pp. 714–723, 2015, doi: 10.1080/1023666X.2016.1081134.

[11] Y. Chen, X. Chen, Y. Liang, and Y. Gao, "Synthesis of polyaspartic acid-oxidized starch copolymer and evaluation of its inhibition performance and dispersion capacity," *J. Dispers. Sci. Technol.*, vol. 42, no. 13, pp. 1926–1935, Nov. 2021, doi:10.1080/01932691.2020.1791172.

[12] Y. Zhou, J. Wang, and Y. Fang, "Green and High Effective Scale Inhibitor Based on Ring-Opening Graft Modification of Polyaspartic Acid," *Catalysts*, vol. 11, no. 7, p. 802, Jun. 2021, doi: 10.3390/catal11070802.

[13] M. F. Mady, A. Rehman, and M. A. Kelland, "Synthesis and Study of Modified Polyaspartic Acid Coupled Phosphonate and Sulfonate Moieties As Green Oilfield Scale Inhibitors," *Ind. Eng. Chem. Res.*, vol. 60, no. 23, pp. 8331–8339, Jun. 2021, doi: 10.1021/acs.iecr.1c01473.

[14] D. Zeng, T. Chen, and S. Zhou, "Synthesis of polyaspartic acid/chitosan graft copolymer and evaluation of its scale inhibition and corrosion inhibition performance," *Int. J. Electrochem. Sci.*, vol. 10, no. 11, pp. 9513–9527, 2015.

[15] S. Shi, Y. Wu, Y. Wang, J. Yu, and Y. Xu, "Synthesis and characterization of a biodegradable polyaspartic acid/2-amino-2-methyl-1-propanol graft copolymer and evaluation of its scale and corrosion inhibition performance," *RSC Adv.*, vol. 7, no. 58, pp. 36714–36721, 2017, doi: 10.1039/c7ra06848d.

[16] M. J. Baari, B. Bundjali, and D. Wahyuningrum, "Synthesis of

oligosuccinimide and evaluation of its corrosion inhibition performance on carbon steel in CO2-saturated 1% NaCL solution," *J. Math. Fundam. Sci.*, vol. 52, no. 2, pp. 202–221, 2020, doi:10.5614/j.math.fund.sci.2020.52.2.5.

[17] X. Sun, J. Zhang, C. Yin, J. Zhang, and J. Han, "Poly(aspartic acid)-tryptophan grafted copolymer and its scale-inhibition performance," *J. Appl. Polym. Sci.*, vol. 132, no. 45, pp. 2–9, 2015, doi: 10.1002/app.42739.

[18] S. Zhang, H. Qu, Z. Yang, C. e. Fu, Z. Tian, and W. Yang, "Scale inhibition performance and mechanism of sulfamic/amino acids modified polyaspartic acid against calcium sulfate," *Desalination*, vol. 419, no. May, pp. 152–159, 2017, doi: 10.1016/j.desal.2017.06.016.

[19] J. Chen, L. Xu, J. Han, M. Su, and Q. Wu, "Synthesis of modified polyaspartic acid and evaluation of its scale inhibition and dispersion capacity," *Desalination*, vol. 358, pp. 42–48, Feb. 2015, doi: 10.1016/j.desal.2014.11.010.

[20] H. Huang, Q. Yao, B. Liu, N. Shan, and H. Chen, "Synthesis and characterization of scale and corrosion inhibitors with hyper-branched structure and the mechanism," *New J. Chem.*, vol. 41, no. 20, pp. 12205–12217, 2017, doi: 10.1039/C7NJ02201H.

[21] R. Gunawan, A. Bayu, and D. Nandiyanto, "How to Read and Interpret 1H-NMR and 13C-NMR Spectrums," *Indones. J. of Sci. & Tech*. vol. 6, no. 2, pp. 267–298, 2021, doi: 10.17509/ijost.v6i2.34189.

[22] Y. M. Syah, *Dasar-Dasar Spektroskopi NMR Satu dan Dua Dimensi*, 1st ed. Bandung: Institut Teknologi Bandung, 2016, ISBN: 9786027440319.

[23] Y. M. Syah, *Dasar-Dasar Penentuan Struktur Molekul Berdasarkan Data Spektrum 1H & 13C NMR*. Bandung: Institut Teknologi Bandung, 2016. ISBN: 9786027440302.

[24] I. W. J. Still, N. Plavac, D. M. McKinnon, and M. S. Chauhan, "Carbon-13 nuclear magnetic resonance spectra of organic sulfur compounds. Comparison of chemical shifts for carbonyl and thiocarbonyl compounds in the pyrone, thiopyrone, and pyridone series," *Can. J. Chem.*, vol. 54, no. 2, pp. 280–289, 1976, doi: 10.1139/v76-042.

[25] Y. Cheng, X. Guo, X. Zhao, Y. Wu, Z. Cao, Y. Cai, & Y.Xu, "Nanosilica modified with polyaspartic acid as an industrial circulating water scale inhibitor," *npj Clean Water*, vol. 4, no. 1, pp. 1–8, 2021, doi: 10.1038/s41545-021-00137-y.

[26] Y. Zhang, H. Yin, Q. Zhang, Y. Li, and P. Yao, "Synthesis and characterization of novel polyaspartic acid/urea graft copolymer with acylamino group and its scale inhibition performance," *Desalination*, vol. 395, pp. 92–98, Oct. 2016, doi: 10.1016/j.desal.2016.05.020.

[27] P. A. Clausen, V. Kofoed-Sørensen, A. W. Nørgaard, N. M. Sahlgren, and K. A. Jensen, "Thermogravimetry and mass spectrometry of extractable organics from manufactured nanomaterials for identification of potential coating components," *Materials (Basel).*, vol. 12, no. 22, pp. 1–21, 2019, doi: 10.3390/ma12223657.

[28] Y. Xi, W. Martens, H. He, and R. L. Frost, "Thermogravimetric analysis of organoclays intercalated with the

surfactant octadecyltrimethyl ammonium bromide," *J. Therm. Anal. Calorim.*, vol. 81, no. 1, pp. 91–97, 2005, doi: 10.1007/s10973-005-0750-2.

[29] T. Chitsiga, M. O. Daramola, N. Wagner, and J. Ngoy, "Effect of the Presence of Water-soluble Amines on the Carbon Dioxide (CO2) Adsorption Capacity of Amine-grafted Poly-succinimide (PSI) Adsorbent During CO2 Capture," *Energy Procedia*, vol. 86, pp. 90–105, Jan. 2016, doi: 10.1016/j.egypro.2016.01.010.

[30] A. Kumar, "Polyaspartic Acid – A Versatile Green Chemical," *Chem. Sci. Rev. Lett. (CSRL), 2012 ,1(2) , pp1-7*, vol. 1, Dec. 2012.